Structural Coupling of Troponin C and Actomyosin in Muscle Fibers†

Hui-Chun Li and Piotr G. Fajer*

Department of Biological Science and National High Magnetic Field Laboratory, Florida State University, Tallahassee, Florida 32306

Received August 20, 1997; Revised Manuscript Received February 20, 1998

ABSTRACT: EPR of spin labeled TnC at Cys98 was used to explore the possible structural coupling between TnC in the thin filament and myosin trapped in the intermediate states of ATPase cycle. Weakly attached myosin heads (trapped by low ionic strength, low temperature and ATP) did not induce structural changes in TnC as compared to relaxed muscle, as spin labeled TnC displayed the same narrow orientational distribution [Li, H.-C., and Fajer, P. G. (1994) *Biochemistry 33*, 14324]. Ca^{2+}-binding alone resulted in disordering of the labeled domain of TnC. Additional conformational changes of TnC occurred upon the attachment of strongly bound, prepower stroke myosin heads (trapped by AlF_4^-). These changes were not present in ghost fibers which myosin had been removed, excluding direct effects of AlF_4^- on the orientation of TnC in muscle fibers. The postpower stroke heads (rigor·ADP/Ca^{2+} and rigor/Ca^{2+}) induced further changes in the orientational distribution of labeled domain of TnC irrespective of the degree of cooperativity in thin filaments. We thus conclude that troponin C in thin filaments detects structural changes in myosin during force generation, implying that there is a structural coupling between actomyosin and TnC.

Muscle contracts when the thick and thin filaments slide past each other to relieve the strain generated by the interaction of the globular head of myosin with actin. In vertebrate skeletal muscle, the thin filament proteins—actin, tropomyosin (Tm),[1] and troponin (Tn)—regulate contraction. The functional regulatory unit is made up of one Tn−Tm complex with seven actin monomers. Troponin is composed of three subunits, each with a distinct function: TnC binds Ca^{2+}, TnI inhibits actin activated myosin ATPase, and TnT binds to tropomyosin (*reviewed in* refs *1*−*3*). Muscle contraction is initiated by Ca^{2+}-binding to the two low-affinity sites of TnC; the signal is then relayed to Tm via TnI and TnT. It is thought that troponin I acts as a switch, by moving away from actin toward troponin C, following Ca^{2+} binding to TnC (*4*, *5*). As the binding of myosin heads to actin also initiates contraction even in the absence of Ca^{2+}, there is a strong possibility that the information flow is bi-directional: from TnC to myosin and from myosin to TnC (*6*−*8*). Structural changes in troponin C initiated by binding of myosin heads have been detected by fluorescence (*9*, *10*) and by electron paramagnetic resonance (*11*). Interestingly, these myosin head induced changes are distinct from those initiated by Ca^{2+}-binding to TnC. The object of the current effort is to characterize the possible structural coupling between the myosin intermediate states and TnC molecules.

Our approach is to trap various actomyosin intermediate states with nucleotide analogues known to induce physically distinct myosin conformations. On the basis of myosin head orientation and mobility and affinity for actin in the skinned muscle fibers, at least five different myosin intermediate states of the ATPase cycle have been identified. For example, the initial, weak binding of the heads to actin leaves the myosin heads disordered and mobile (*12*, *13*). The weakly bound myosin heads can isomerize to a strongly bound state with decreased mobility, but the binding to actin is not stereospecific insofar that the heads are disordered (*14*). The *disorder-to-order transition* of the strongly bound heads might be the key step for force generation (*14*, *15*). The myosin heads in states following the release of phosphate are well ordered and immobilized on a microsecond time scale (*16*, *17*). However, in the presence of ADP, there is a substantial conformational heterogeneity accompanied by a slow "breathing" motion of the catalytic domain (*14*). The release of ADP from myosin active site dampens the local domain motions of the catalytic domain.

Here, we compared the behavior of labeled TnC with different myosin intermediate states and have found that the orientational distribution of TnC is not affected by the binding of myosin heads in the "weak" states (see Scheme 1), but is sensitive to the binding of strongly attached heads.

† This project was supported by grants from American Heart Association Grant GIA-9501335 and from National Science Foundation Grant IBN-9507477 to P. F. This work was presented at the Biophysical Society meeting in Baltimore, 1996.

* To whom correspondence should be addressed. E-mail: fajer@magnet.fsu.edu.

[1] Abbreviations: A, actin; ADP, adenosine-5′-diphosphate; ATP, adenosine-5′-triphosphate; BDM, 2,3-butanedione monoxime; DTT, dithiothreitol; EDTA, ethylenediamine tetraacetic acid; EGTA, ethylene glycol-bis(β-aminoethyl ether) *N*,*N*,*N*′*N*′-tetraacetic acid; EPR, electron paramagnetic resonance; M, myosin; MSL, *N*-(1-oxy-2,2,5,5-tetramethyl-4-piperidinyl)maleimide; S1, myosin subfragment 1; TM, tropomyosin; Tn, troponin; TnC, troponin C; TnI, troponin I; TnT, troponin T.

S0006-2960(97)02062-X CCC: $15.00
Published on Web 04/22/1998

Scheme 1

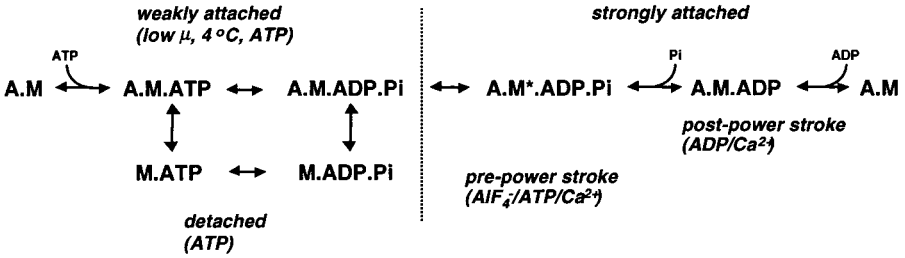

Moreover, the structural change of TnC induced by the prepower stroke heads (trapped by AlF_4^-) is different from that induced by the postpower stroke (rigor·ADP and rigor)[2] heads. The difference between the effects induced by the prepower and postpower stroke states strongly suggests that the force generating structural changes in the actomyosin complex are accompanied by structural changes in troponin C.

MATERIALS AND METHODS

Sample Preparation

Skinned rabbit psoas fibers were prepared and stored as described previously by Li and Fajer (*11*). Skeletal TnC was purified from rabbit back and leg muscle according to the method of Potter (*18*). Cys98 in TnC was labeled with a 3-fold excess of *N*-(1-oxy-2,2,6,6-tetramethyl-4-piperidinyl)maleimide (MSL) (Aldrich Chemical Co., Milwaukee, WI) at ~25 μM of TnC in 20 mM HEPES, 0.1 M KCl, 2 mM EDTA, pH 7.5, for 4 h at 20 °C. Endogenous TnC was extracted from skinned fibers with EDTA and was then replaced with labeled TnC according to Moss (*19*). The extent of the TnC reconstitution was better than 95% as determined by densitometry of SDS gels of fiber segments. The Ca^{2+} activated force, which was totally abolished after TnC removal, is fully recovered on addition of spin labeled TnC (*11*).

The chemical states of the myosin heads were controlled by the buffer composition. Rigor buffer (RB) consisted of 130 mM KPr, 2 mM $MgCl_2$, 1 mM EGTA, 20 mM MOPS, and 1 mM NaN_3, pH 7.0. Relaxation was achieved by adding 5 mM MgATP to RB, while the activating solution contained 5 mM MgATP plus 1.5 mM $CaCl_2$. Low ionic strength relaxing buffer has the same composition as the relaxation buffer but with no salt, resulting in an ionic strength $\mu = 0.03$ M (*12*). The ADP solution contained 4 mM MgADP, 100 μg/mL hexokinase (Sigma, St. Louis, MO), 10 mM glucose, and 100 μM AP_5A ((*P*^{1},*P*^{5}-bis(5′-adenosyl)pentaphosphate) (Boehringer, Indianapolis, IN) in RB (*17*). Aluminum fluoride solution was prepared by the addition of 10 mM NaF and 1 mM $AlCl_3$ to activating buffer (*20*). A stock solution of 100 mM V_i was prepared by dissolving Na_3VO_4 in H_2O and adjusting the solution to pH 10 with 6 N HCl. The solution was then boiled until colorless, followed by rechecking the pH of the cooled solution (*21*). BDM (2,3-butanedione 2-monoxime) powder was added directly to the RB with 5 mM V_i solution, to make a final concentration of 50 mM BDM (*22*).

Ghost fibers were prepared by incubation of TnC-depleted fiber bundles with Hasselbach−Schneider solution (10 mM MOPS, 1 mM EGTA, 600 mM KCl, 0.5% Triton, and 5 mM MgATP, pH 7.0) for 30 min to depolymerize the intrinsic myosin. Sarcomere length of our fiber preparations was 2.41 μm. The fibers are held isometrically to prevent any length changes between solutions.

Electron Paramagnetic Resonance

MSL−TnC reconstituted fibers (0.5 mm diameter) were placed in 1-mm glass capillaries (50 μL, VWR Scientific, Marietta, GA) and held isometrically by surgical silk thread (no. 6; Deknatel, Fall River, MA) that was tied to the ends of the fiber bundle. Solutions were continuously flowed over the fibers at a rate of 0.5 mL/min, controlled by a peristaltic pump (P3, Pharmacia, Piscataway, NJ). EPR experiments were performed on a Bruker ECS-106 spectrometer (Bruker Inc., Billerica, MA), using a modified TM_{110} cavity allowing sample placement parallel to the static magnetic field. Conventional EPR spectra were recorded at a microwave power of 0.032 G microwave field and a modulation field of 2.5 G. All experiments were performed at room temperature (21 °C) except for low ionic strength relaxation performed at 4° C. Spectra were acquired, averaged, and analyzed using an IBM-compatible personal computer with spectral analysis software developed in our laboratory (*23*). The full width at half-maximum height of the low (ΔL) and high (ΔH) field peaks of the experimental spectra were determined from the least-squares fit of the spectrum to the sixth order polynomial (Excel, Microsoft Inc, Redmond, WA). The correlation coefficient in all cases was better than 0.99.

Mechanical Measurements

Fiber stiffness was measured using a force transducer and a length driver (Cambridge Technology, Watertown, MA), interfaced to a personal computer, and controlled by a DAC program (University of Washington Seattle). For each measurement, the fiber length was changed in steps of 0.3, 0.5, 0.7, 0.9, and 1.1% of the fiber length. The steps were completed within 0.3 ms. Since the fiber states of interest were not generating force, the measurement was delayed till 12 ms after the step to allow the decay of the mechanical ringing present in our system.

RESULTS

To examine the orientational distribution of MSL−TnC[3] in various myosin states, we trapped the intermediate states

[2] A similar observation based on linear dichroism of labeled TnC was reported by Martyn, Chase and Gordon at the Actin Binding Proteins conference, Maui, 1997.

[3] Although we are observing the behavior of a specific site in troponin C (Cys98), for the sake of brevity we will refer to the orientational distribution of TnC.

Table 1: Spectral Parameters of Fibers Reconstituted with MSL−TnC in Various Intermediate States of Myosin Cross-Bridges

cross-bridge states	$2T_{eff}$ (G)[a]	ΔL (G)[b]	ΔH (G)[b]	no. of experiments
relaxed	69.8 ± 0.6	4.3 ± 0.1	5.4 ± 0.5	6
weakly bound	70.3 ± 0.1	4.4 ± 0.1	5.4 ± 0.1	2
rigor·ADP/Ca^{2+}	63.7 ± 0.6[c]	6.3 ± 0.3	9.8 ± 0.8	5
rigor/Ca^{2+}	65.5 ± 0.6	6.3 ± 0.3	9.9 ± 0.5	15
AlF_4^-/ATP/Ca^{2+}	65.5 ± 0.5	6.2 ± 0.3	8.4 ± 0.4	11
Vi/BDM/ATP/Ca^{2+}	65.8 ± 0.5	6.6 ± 0.2[d]	9.5 ± 0.4[e]	11

[a] $2T_{eff}$, the separation between the outermost peaks. [b] ΔL and ΔH, full width at half-height of the low- and high-field peaks determined from the polynomial fit. [c] $p = 0.016$ for $2T_{eff}$ between rigor·ADP/Ca^{2+} and rigor/Ca^{2+} states. [d] $p = 0.034$ for ΔL between Vi/BDM/Ca^{2+} and rigor/Ca^{2+} states. [e] $p < 0.001$ for ΔH between Vi/BDM/Ca^{2+} and rigor/Ca^{2+} states.

of myosin ATPase with various chemical analogues (see Scheme 1). Weakly attached states (a) were trapped with ATP at low ionic strength and low temperature, or in the presence of vanadate and BDM; (b) the strongly attached prepower stroke state was induced in the presence of AlF_4^-, ATP and Ca^{2+}; (c) the postpower stroke states were attained with ADP and Ca^{2+}, and with rigor and Ca^{2+}.

Our previous work with maleimide spin-labeled TnC has established the rigidity of the label with respect to the protein in TnC reconstituted muscle fibers. Conventional EPR spectra of randomly oriented samples (myofibrils) and saturation transfer EPR experiments showed that the spin label is immobilized on the nanosecond time scale of the experiments presented below and on the millisecond time scale of the ST-EPR experiments (*11*, *24*). Thus the spectral changes which we report below are due to changes in the orientational distribution of the labeled domain at Cys98 of TnC and not due to motion of the label with respect to the protein.

(a) Relaxed State. In the relaxed state, the EPR spectrum of reconstituted MSL−TnC is characterized by its large splitting ($2T_{eff}$ = 69.8 ± 0.6 G, Table 1). The negative intensity at *L**, as well as the peak at *H**, is indicative of a small degree of order in the pseudopowder line shape of Figure 1a. Spectral simulations suggest that this spectrum is composed of two line shapes, corresponding to two spin populations which have angular distributions centered at 22° and 58° with respect to the fiber axis and a Gaussian disorder about the average angles of 14° and 27°, respectively (*11*). The origin of the two populations is most likely due to the rotational isomerization of Cys98 as observed in the crystal structures (*25*, *26*), which might persist after reconstitution of TnC into fibers. The high degree of order in TnC is contrasted with disordering of the detached heads in relaxation (*27*).

(b) Weakly Bound State. The initial, transient attachment of myosin heads to actin is achieved by relaxation at low ionic strength and low temperature (*28*). The heads are in a rapid equilibrium between attached and detached cross-bridges, favoring the latter by 2:1. Initial binding is not stereospecific, the heads are disordered and mobile yet they are different from those in relaxation (*12*, *13*). The weakly bound state, although induced by nonphysiological conditions, is an intermediate state of the actomyosin cycle in muscle fibers (*29*). As seen in Figure 1, the effect of these weakly attached cross-bridges on the orientation of MSL−TnC in fibers is unnoticeable. The line shape of the spectrum at low ionic strength (Figure 1b) is the same as that in the fully relaxed state at physiological ionic strength (Figure 1a). Statistical analysis (*t*-test) confirms this conclusion; there is no significant difference of the diagnostic spectral parameters—the effective hyperfine splitting ($2T_{eff}$) and the full-widths of low- and high-field region resonances (ΔL and ΔH) remain unchanged (Table 1).

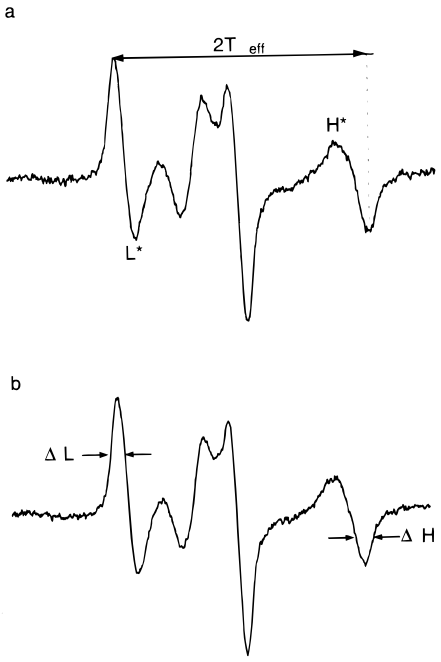

FIGURE 1: The EPR spectra of MSL labeled TnC (a) in relaxed fibers, 23° C, and (b) fibers relaxed in low ionic strength buffer, 4° C. Total scan width is 120 G.

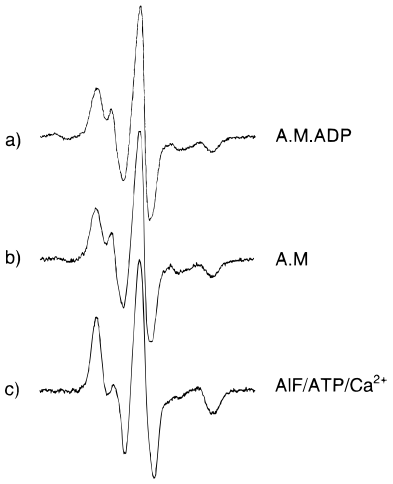

FIGURE 2: The EPR spectra of MSL labeled TnC reconstituted fibers with strongly bound cross-bridges: (a) in the presence of MgADP and Ca^{2+}, (b) rigor cross-bridges with Ca^{2+}, and (c) in the presence of AlF_4^-, ATP, and Ca^{2+}.

(c) Rigor·ADP/Ca^{2+} State. The rigor·ADP state is thought to be an analogue of the strongly bound postpower stroke state (*30*, *31*). Myosin heads are well ordered and immobilized albeit with a local domain heterogeneity and dynamics (*14*). This is not the case for labeled TnC. The spectrum of MSL−TnC in fibers in the rigor·ADP/Ca^{2+} state (Figure 2a) is similar to the spectra of minced muscle fibers which are completely random. The splitting of 63.7 ± 0.6 G (Table 1) is about 6 G smaller than the $2T_{eff}$'s of relaxed

and weakly bound states, implying that the center of the orientational distribution of nitroxide attached to TnC is more perpendicular to the fiber axis than the distribution in relaxed state. The resonance widths ΔL and ΔH are 6.3 and 9.8 G, significantly larger than those of the relaxed or weakly bound states, $\Delta L = 4.3$ and $\Delta H = 5.4$ G (Table 1). Thus, the attachment of strongly bound heads causes a large change in orientational distribution of TnC.

(d) Rigor/Ca^{2+} State. The release of ADP to form rigor cross-bridges results in a small (<7°) twisting movement of the head (*23*, *32*) accompanied by the inhibition of the local domain motions (*14*). The presence of Ca^{2+} has no effect on either the orientation or mobility of the catalytic domain of myosin (Adhikari, private communication). The spectrum of MSL−TnC in fibers in the rigor/Ca^{2+} state (Figure 2b) has the same spectral features as the spectrum in rigor·ADP/Ca^{2+} state (Figure 2a). The diagnostic parameters $2T_{eff}$, ΔL, and ΔH of these two myosin states are within experimental error (Table 1). Thus, the conformational changes in the catalytic domain of myosin induced by ADP release are not accompanied by an observable reorientation of TnC. We want to emphasize that the MSL−TnC spectrum in the rigor/Ca^{2+} state is different from that in the rigor state in the absence of calcium. Calcium binding to rigor fibers induces an additional, five-degree rotation of the labeled domain of TnC (*11*).

(e) AlF_4^-/ATP/Ca^{2+} State. The complex of A·M·ADP and aluminum fluoride ion (AlF_4^-) is an analogue of the prepower stroke state: A·M*·ADP·Pi (*33*, *34*). In muscle fibers, AlF_4^- causes 100% inhibition of force generation and only a 60% decrease of stiffness, indicating entrapment of a large fraction of heads in the prepower stroke, strongly bound state (*35*). Myosin heads in this state are as disordered as in relaxation with no sign of rigor or ADP-like orientation, yet their mobility is severely diminished (*20*, 36). This disordering of the strongly attached heads reflects a non-stereospecific actomyosin complex in the prepower stroke state from which an ordering rotations ending in a well-ordered ADP state might generate force.

Aluminum fluoride ion (AlF_4^-) is also known to interact directly with isolated TnC in solution (*37*); the effects included a change in the degree of TnC helicity and exposure of the hydrophobic patch involved in TnI binding. As pointed out by Phan and Reisler (*37*), any effect observed by spectroscopic probes on TnC can, in principle, be due to AlF_4^- binding to TnC rather than trapping of myosin head in the intermediate state of the cycle. To exclude this possibility in muscle fibers in which TnC is complexed with other troponin subunits, we have compared the spectra of MSL−TnC reconstituted ghost fibers with and without AlF_4^-. As the myosin is removed from ghost fibers, all effects will be that of AlF_4^- binding to TnC. As seen in Figure 3a, no spectral changes were observed, demonstrating that AlF_4^- did not alter the orientation of TnC in the absence of myosin heads. Moreover, AlF_4^- did not induce any spectral changes in the presence of rigor cross-bridges and Ca^{2+} (Figure 3b). It seems that the changes previously observed for the isolated TnC molecules in solution (*37*) are not occurring in the troponin complex reconstituted into muscle fibers.

The effects of AlF_4^- trapped intrinsic heads are shown in Figure 2c. The comparison of the spectra in AlF_4^-/ATP/Ca^{2+} and rigor/Ca^{2+} states revealed a small but significant difference in the spectral splitting (Table 1) and in the width of high-field resonances (Figure 4). The high field peak of the spectrum in AlF_4^-/ATP/Ca^{2+} state ($\Delta H = 8.4 \pm 0.4$ G) is sharper than that in the rigor/Ca^{2+} state ($\Delta H = 9.9 \pm 0.5$ G), implying a distinct orientational distribution (confidence $p < 0.001$, Table 1).

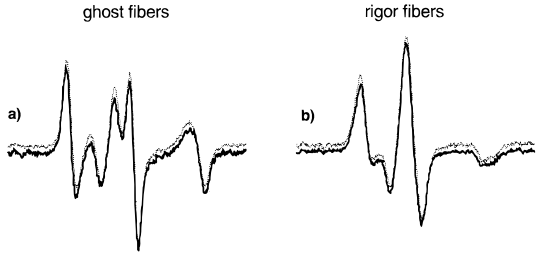

FIGURE 3: The EPR spectra of MSL−TnC-reconstituted fibers in the presence (solid line) and the absence (dotted line) of AlF_4^-. (a) Myosin-extracted ghost fibers; (b) fibers in the rigor/Ca^{2+} state. Spectra are offset for comparison.

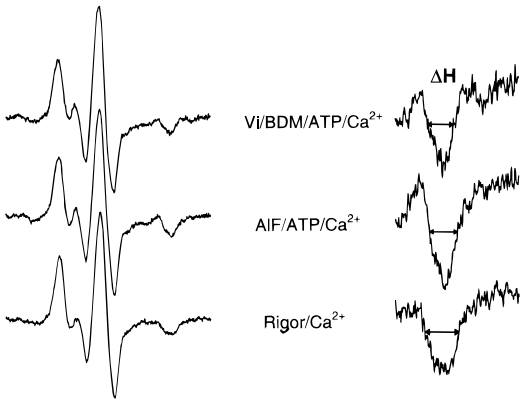

FIGURE 4: Comparison of EPR spectra of MSL−TnC reconstituted fibers in Vi/BDM/ATP/Ca^{2+} state, AlF_4^-/ATP/Ca^{2+} state, and rigor/Ca^{2+} state. The high field region of the spectra is magnified to show the differences in ΔH (Table 1). These spectra are obtained from the same fiber bundles.

If the conformation of TnC is homogeneous along the thin filament length in this state, then we can conclude that its conformation is different in the prepower stroke and post-power stroke states. However, since only a fraction (20−40%) of the AlF_4^- trapped heads binds to actin in fibers, two populations of TnC can be expected: those in the vicinity of the attached heads and those in the vicinity of detached or weakly attached heads. The relative fraction of each population depends on the degree of cooperativity. Thus, we expect that the AlF_4^-/ATP/Ca^{2+} spectrum is a sum of two line shapes: (a) the TnC line shape activated by Ca^{2+} in the presence of the detached or weakly attached heads and (b) a spectrum of TnC seeing both Ca^{2+} and prepower stroke cross-bridges. To determine the spectral line shape of the former component (a) (TnC in the neighborhood of weakly attached heads but in the presence of Ca^{2+}), we added BDM and vanadate to the activating solution (ATP and Ca^{2+}). BDM reduces the isometric tension, shortening speed and instantaneous stiffness of fibers (*22*, *38*), while vanadate inhibits the myosin ATPase activity by forming a complex that is believed to mimic either the transition state of hydrolysis or the ADP·Pi state (*21*, *39*). The tension generated by fibers in the presence of 5 mM Vi, 50 mM BDM, ATP, and Ca^{2+} was less than 2% of the active tension,

Table 2: Fiber Stiffness and Tension

state	stiffness (% fraction of rigor)[a]	tension (% fraction of contraction)[a]
rigor	100	
relaxation	6 ± 1	0
contraction	55 ± 7	100
ATP/AlF_4^-/Ca^{2+}	43 ± 3[b]	<5[b]
Vi/BDM/ATP/Ca^{2+}	11 ± 1	<5

[a] Errors are SEM from 8 independent measurements. [b] From ref 20.

and the stiffness was 11% of the rigor stiffness (Table 2). These low values indicate that very few myosin heads are bound to actin filament. If the thin filament compliance is taken into account, only 4−9% of the heads are strongly bound to actin, as estimated from $n(x) = 0.5x/(0.5 + x)$, where n is the number of attached cross-bridges and x is the normalized stiffness (*40*). This small fraction of the heads is unlikely to fully activate the thin filament. Trybus and Taylor (*41*) estimated that attachment of 2 or 3 rigor heads is needed for activation of a regulatory unit (seven actin monomers).[4] Additionally, the spread of activation along the thin filament is limited to a very short range (*42*, *43*).

The second (b) component of the linear combination is of interest here; this is *the component* originating from TnC affected by the prepower stroke heads. If this component was the same as the postpower stroke line shape, then the composite spectrum should be a linear combination of rigor/Ca^{2+} and Vi/BDM/Ca^{2+} spectra. The width of the high-field resonance peak of the composite spectrum should then be: $\Delta H_{AlF_4^-/ATP/Ca^{2+}} = (1 - x)\,\Delta H_{Vi/BDM/Ca^{2+}} + x\Delta H_{Rigor/Ca^{2+}}$, where the subscripts denote the fiber conditions and x is the fraction of TnC affected by the strongly bound heads. This fraction is not known a priori because the binding of cross-bridges to regulated actin filaments is cooperative (*44*) but the extent of cooperativity in the presence of AlF_4^- is not known. Nevertheless, the value of x must be between 0 and 1 if the spectrum is a linear combination of the spectra in the two states, resulting in an intermediate line width, smaller than $\Delta H_{Rigor/Ca^{2+}}$ value but larger than the $\Delta H_{Vi/BDM/Ca^{2+}}$. However, this was not the case for the observed spectra (Table 1), the line width in the presence of AlF_4^- (8.4 ± 0.4 G) is smaller than that for both detached and postpower stroke cross-bridges (9.5 ± 0.4 and 9.9 ± 0.5 G). Therefore, the spectrum in AlF_4^-/ATP/Ca^{2+} state is not a linear combination of a spectrum in Vi/BDM/ATP/Ca^{2+} and a spectrum in rigor/Ca^{2+} state, which in turn implies that the prepower stroke cross-bridges induce a different structure of TnC from that induced by the postpower stroke cross-bridges (rigor·ADP/Ca^{2+} and rigor/Ca^{2+}).

We conclude that TnC senses structural change in the thin filaments which accompany the structural changes within the myosin head during ATP hydrolysis and force generation.

[4] Alternative state mimicking the detached weakly attached cross-bridges in the presence of Ca^{2+} is the state induced by ATPγS/Ca^{2+}. However, the EPR spectra of muscle fibers with spin label on myosin suggest the presence of ∼17% fraction of ADP (rigor) heads (*74*). These heads can, in principle, activate the whole thin filament. Therefore, the ATPγS/Ca^{2+} would not be as good control as Vi/BDM/Ca^{2+} cocktail.

DISCUSSION

In this study we attempted to correlate the conformational states of TnC with the intermediate states of myosin in muscle fibers. Although quantitative description of the orientational distribution of each TnC state was not possible due to large disorder, the statistically significant spectral differences clearly point to the differences in the orientation of the spin labeled domain (Cys98) in TnC. The results show that: (a) the strongly bound, but not weakly bound, cross-bridges induce reorientation of TnC; (b) the conformation of TnC induced by the strongly bound prepower stroke heads is different from that induced by the postpower stroke heads; and (c) the release of ADP from myosin does not result in reorientation of TnC. Taken together, these findings give a strong credence to the proposed structural coupling orientation between myosin and regulatory proteins and to the notion that the TnC is *"not a simple on−off switch"* (*10*).

More subtle coupling between the intermediate states of myosin and TnC was demonstrated by Zot and Potter (*45*) and Morano and Ruegg (*46*) who showed that fluorescence intensity of labels attached to the N-domain of TnC is a function of the nucleotide state of myosin catalytic domain. The fluorescence intensity changes are difficult to interpret, as they can be brought on by a number of structural events resulting in quenching or changes in environment polarizability. Though electron paramagnetic resonance is a less sensitive technique, the results are less ambiguous to interpret. In general, EPR spectra are determined by the nanosecond mobility of the spin label. If the label's motion is slow (rotational correlation time greater than 200 ns) as is the case here, the spectra of ordered samples are defined by the average orientation of the spin label and its disorder. Therefore, an observed spectral change from an ordered sample (e.g., muscle fibers) can be interpreted as a structural change of the labeled domain. Thus, the main contribution of this study is in finding a structural correlate—orientational distribution—which accompanies the thick−thin filament coupling observed by Potter and his collaborators.

The proposed structural coupling is not limited to TnC, it involves tropomyosin and actin. Ishii and Lehrer (*47*) showed that the excimer fluorescence of pyrene attached to tropomyosin is sensitive to weak−strong transition of myosin cross-bridges whereas Wakabayashi et al. (*48*) reported changes in actin layer lines of X-ray diffraction patterns between the cycling and rigor cross-bridges. Thus, it is very likely that the multiple structural events involving actin, tropomyosin, and troponin complex are all part of the pathway coupling myosin and regulatory proteins.

Biochemical manifestations of the structural coupling between myosin and TnC are well established: binding of rigor S1 increases TnC affinity for Ca^{2+} (*6*, *8*, *42*) and conversely Ca^{2+} binding to TnC stimulates transition from weak-to-strong binding of S1 in reconstituted thin filaments (*7*). Each of the ligands binds cooperatively to their target sites, Ca^{2+} to TnC (*49*, *50*) and S1 to actin (*7*, *51*). The cooperativity of binding to one ligand is affected by the binding of another ligand: the cooperativity of S1 binding to actin decreases in the presence of Ca^{2+} (*7*), and the cooperativity of Ca^{2+} binding to TnC decreases on S1 binding to actin (*10*).

The effects on ligand binding are accompanied by the effects on the enzymatic activity. Actomyosin ATPase is fully activated only at high levels of S1 saturation even in the presence of Ca^{2+} (*52*).[5] Finally, the coupling is visible at the functional level−force generation in whole muscle fibers. Increase in the population of weak states in isometrically contracting muscle fibers decreases pCa for half-force development rendering the muscle less sensitive to Ca^{2+} (*53*, *54*). Increase of the fraction of strongly bound heads (A·M·ADP) resulted in increased Ca^{2+} sensitivity of force (*53*). Activation of the thin filaments by strong binding cross-bridges in muscle fibers was also observed in studies of force recovery after length release (*55*) and kinetics of force depression after photolysis of caged Pi (*54*, *56*). Taken together, all the structural, biochemical, and fiber mechanics observations point to a structural correlation between thick and thin filament proteins which might form the basis for the coupling between force generating events and force regulation.

Two different mechanisms have been proposed for thin filament regulation: a steric block mechanism based on structural studies of muscle fibers (*57*−*59*) and an allosteric/kinetic model based on kinetic and equilibrium studies of isolated proteins (*7*, *60*, *61*). In the steric blocking model, calcium binding to TnC induces an azimuthal movement of tropomyosin on the thin filament, away from a position covering myosin binding sites. The overlap of tropomyosin's position and the myosin binding site on actin, in the absence of Ca^{2+}, has been confirmed by the structural studies of Flicker et al. (*62*), Lehman et al. (*63*), Lorenz et al. (*64*), and Vibert et al. (*65*). In the kinetic model, Ca^{2+} does not regulate the binding of myosin heads to thin filaments but rather accelerates a kinetic transition of the bound heads from a nonforce producing state to a force producing state. Both schemes can be reconciled by the recent models of Geeves and Lehrer (in refs *1*, *2*). McKillop and Geeves (*66*) proposed that the thin filament is in rapid equilibrium between three states, defined functionally by the state of myosin head: *blocked*, which does not bind myosin; *closed*, which binds myosin weakly and *open*, in which the weakly bound myosin can isomerize to the strongly bound conformation. Force is generated in the thin filament open state during the myosin head weak-to-strong transition. Structurally, the state of the thin filament is determined by the position of tropomyosin and the actomyosin interface, and it is different for weakly binding and for strongly binding cross-bridges. The position of tropomyosin on the actin determined by X-ray diffraction supports Geeves's three-state model (*67*, *68*). In the absence of Ca^{2+}, Tm blocks myosin binding but allows weak interaction with actin (*blocked state*); in the presence of Ca^{2+}, tropomyosin still prevents full actomyosin interaction (*closed state*); a further movement of Tm is necessary for the full rigor interaction (*open state*). These findings were confirmed by the reconstruction of thin filament by electron microscopy. Vibert and colleagues (*65*) observed a 25° rotation of Tm on binding of Ca^{2+} exposing most (but not all) S1 binding site, with a further 10° shift induced by myosin binding.

[5] Synergistic effects of S1 and Ca^{2+} were observed on structural level, with fluorescence (*10*, *45*) and with EPR (*11*) probes.

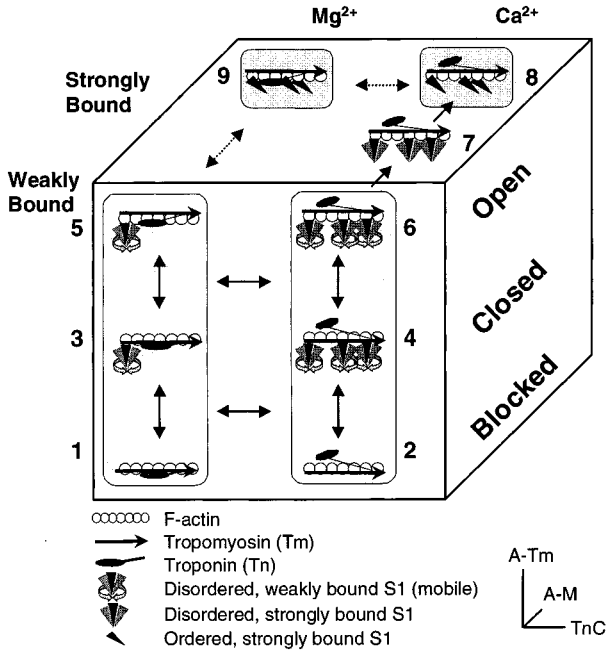

FIGURE 5: A modified scheme from Lehrer (1994) illustrates the three types of thin filament regulations. The dimensions are ascribed to different regulatory components. *x*-axis, troponin C with Mg^{2+} and Ca^{2+} states; *y*-axis, actin−myosin interaction with weakly bound and strongly bound cross-bridges; *z*-axis, actin−tropomyosin with *blocked*, *closed*, and *open* states. Each state is numbered, and each box represents a distinct MSL−TnC conformation.

In the models described above, the TnC/Tn complex has been regarded as an "all-or-nothing" Ca^{2+} switch, coupled to the state of tropomyosin. More recently, a "three two-state system" model with separate regulation of troponin and tropomyosin was presented by Lehrer (*1*). In Lehrer's model, the thin filament is regulated by three distinct protein systems each with binary states: *on*−*off* states of actin−tropomyosin, *Mg*$^{2+}$ and *Ca*$^{2+}$ states of troponin, and *weakly*−*strongly* bound states of the myosin heads. In Figure 5 we have redrawn Lehrer's scheme to include the three states of the actin−tropomyosin complex (*blocked*, *closed*, and *open*). When Tm is in the *blocked* state the myosin heads do not bind actin significantly, but Ca^{2+} binding to TnC induces a conformational change of TnC in muscle fibers (states 1 and 2 in Figure 5, *9*, *11*, *45*). Tropomyosin does not interfere with the weak binding of myosin to actin in the *closed* states (states 3 and 4), but sterically interferes with the strong binding heads. In the *open* states (states 5 and 6), Tm moves to another position on actin thus allowing weakly bound cross-bridges to isomerize to strongly bound states (states 6−8).

The conformation of TnC in actin-Tm *closed*/*open* states in the absence of Ca^{2+} (states 3 and 5, Figure 5) has been explored with fluorescence spectroscopy. Morano and Ruegg (*46*) showed that weakly bound cross-bridges induce an intensity change of danzylaziridine (DANZ) fluorescence. Here, we were not able to detect any orientational change of MSL−TnC induced by weakly attached cross-bridges under the same conditions. The different regions of TnC probed in the two experiments are at the root of the apparent discrepancy: the N-terminal domain in the fluorescence study (Met25) and the C-terminal domain (Cys98) probed here. The two domains of TnC have different roles: the C-terminal domain anchor TnC to the thin filament and the N-terminal

domain transmits the Ca^{2+} signal (*3*, *69*). Thus, it is not surprising that the two domains respond differently to ligand binding.

The identical orientational distribution of MSL−TnC in the *blocked* state (Figure 5, state 1) and in the *closed/open* states (Figure 5, states 3 and 5) implies that the state of tropomyosin does not influence the structure of C-terminal of TnC. This lack of structural coupling between Tm and TnC is reciprocal, since the nanosecond mobility of tropomyosin probed at Cys190 is affected little by either Ca^{2+} or S1 in muscle fibers (*70*).

Two additional states have been added to the Lehrer and Geeves's model. The first one is an *open* state of actin−Tm, which is induced by strongly bound rigor cross-bridges in the absence of Ca^{2+} (Figure 5, state 9). Results from both EPR and fluorescence studies have shown that rigor cross-bridges alone induce a conformational change of TnC distinct from that induced by Ca^{2+} (*9*−*11*, *45*). When both Ca^{2+} and rigor cross-bridges are present (Figure 5, state 8), a further conformational change of TnC is observed (*9*−*11*, *45*). A new state identified in this study is an *open* state of actin−Tm. This conformation is induced by strongly bound, prepower stroke myosin heads in the presence of Ca^{2+} (Figure 5, state 7) and is different from that induced by postpower stroke heads in the presence of Ca^{2+} (Figure 5, state 8). As the distinct conformations of TnC are paralleled by the distinct conformations of the pre- and postpower stroke cross-bridges (*14*, *15*, *20*), there seems to be a structural coupling between TnC in the thin filaments and myosin in the thick filament accompanying force generation. The signal transduction pathway, with myosin and TnC at either end and possibly involving actomyosin interface, actin, tropomyosin, and other troponin subunits, could be the structural basis for increased Ca^{2+} affinity of TnC in the presence of attached myosin heads (*10*), changes in acto−myosin affinity (*7*, *41*), and tropomyosin affinity for actin (*71*), culminating in the increased actomyosin ATPase rates (*72*, *73*).

In conclusion, we have demonstrated that strongly bound cross-bridges can induce a structural change in troponin C. The conformation of troponin C induced by prepower stroke cross-bridges is different from that induced by postpower stroke cross-bridges, suggesting a subtle structural coupling in muscle fibers which allows regulatory proteins to sense not only cross-bridge attachment but more importantly force generating transition. One can speculate that the myosin head itself may provide a feedback mechanism for Ca^{2+} initiated regulation of muscle contraction.

ACKNOWLEDGMENT

We thank Dr. Ken Taylor for critically reading the manuscript, Steve Madden for help with the mechanical experiments, Ken Sale for help with data analysis, and Dr. Thomas Palm for purified TnC.

REFERENCES

1. Lehrer, S. S. (1994) *J. Muscle Res. Cell Motil. 15*, 232−236.
2. Tobacman, L. S. (1996) *Annu. Rev. Physiol. 58*, 447−481.
3. Zot, A. S., and Potter, J. D. (1987) *Annu. Rev. Biophys. Chem. 16*, 535−559.
4. Tao, T., Gong, B.-J., and Leavis, P. C. (1990) *Science 247*, 1 339−341.
5. Tao, T., Gowell, E., Strasburg, G. M., Gergely, J., and Leavis, P. C. (1989) *Biochemistry 28*, 5902−5908.
6. Fuchs, F. (1977*) Biophys. Biochem. Acta 462*, 314−322.
7. Greene, L. E., and Eisenberg, E. (1980) *Proc. Natl. Acad. Sci. U.S.A. 77*, 2616−1620.
8. Rosenfeld, S. S. and Taylor, E. W. (1984) *J. Biol. Chem. 259*, 11908−11919.
9. Gordon, A. M., Ridgway, E. B., Yates, L. D., and Allen, T. (1988) *Adv. Exp. Med. Biol. 226*, 89−99.
10. Guth, K., and Potter, J. D. (1987) *J. Biol. Chem. 262*, 13627−13635.
11. Li, H.-C., and Fajer, P. G. (1994) *Biochemistry 33*, 14324−14332.
12. Fajer, P. G., Fajer, E. A., Schoenberg, M., and Thomas, D. D. (1991) *Biophys. J. 60*, 642−649.
13. Yu, L. C., and Brenner, B. (1989) *Biophys. J. 55*, 441−453.
14. Raucher, D., Sar, C. P., Hideg, K., and Fajer, P. G. (1994) *Biochemistry 33*, 14317−14323.
15. Thomas, D. D., Ramachandran, S., Roopnarine, O., Hayden, D. W., and Ostap, E. M. (1995) *Biophys. J. 68*, 135−141s.
16. Thomas, D. D., Ishiwata, S., Seidel, J. C., and Gergely, J. (1980) *Biophys. J. 32*, 873−890.
17. Fajer, P. G., Fajer, E. A., Matta, J. J., and Thomas, D. D. (1990) *Biochemistry 29*, 5865−5871.
18. Potter, J. D. (1982) *Methods Enzymol. 85*, 241−263.
19. Moss, R. L. (1992) *Circ. Res. 70*, 865−884.
20. Raucher, D., and Fajer, P. G. (1994) *Biochemistry 33*, 11993−11999.
21. Goodno, C. C. (1982) *Methods Enzymol. B85*, 116−123.
22. Higuchi, H., and Takemori S. (1989) *J. Biochem. 105*, 638−643.
23. Fajer, P. G. (1994a) *Proc. Natl. Acad. Sci. U.S.A. 91*, 937−941.
24. Li, H.-C., Hideg, K., and Fajer, P. G. (1997) *J. Mol. Recognit. 10*, 194−201.
25. Herzberg, O., and James, M. N. G. (1988) *J. Mol. Biol. 203*, 761−779.
26. Satyshur, K. A., Pyzalska, D., Greaser, M., Rao, S. T., and Sundaralingam, M. (1994) *Acta Crystallogr. D50*, 40−49.
27. Thomas, D. D. and Cooke, R. (1980) *Biophys. J. 32*, 891−906.
28. Brenner, B., Schoenberg, M., Chalovich, J. M., Greene, L. E., and Eisenberg, E. (1982*) Proc. Natl. Acad. Sci. U.S.A. 79*, 7288−72891.
29. Schoenberg, M. (1993) *Adv. Biophys. 29*, 55−73.
30. Dantzig, J. A., and Goldman, Y. E. (1985) *J. Gen. Physiol. 86*, 305−327.
31. Sleep, J. A., and Hutton, R. I. (1980) *Biochemistry 19*, 1276−1283.
32. Fajer, P. G. (1994b) *Biophys. J. 66*, 2039−2050.
33. Maruta, S., Henry, G. D., Sykes, B. D., and Ikebe, M. (1993) *J. Biol. Chem. 268*, 7093−7100.
34. Phan, B. C., Faller, L. D., and Reisler, E. (1993) *Biochemistry 32*, 7712−7719.
35. Chase, P. B., Martyn, D. A., Kushmerick, M. J., and Gordon, A. M. (1993) *J. Physiol. 460*, 231−246.
36. Raucher, D., Fajer, E. A., Hideg, K., Sár, C. P., Zhao, Y., Kawai, M., Fajer, P. G. (1995) *Biophys. J. 68*, 128.
37. Phan, B. C., and Reisler, E. (1993) *Biophys. J. 65*, 2511−2516.
38. Zhao, L., Naber, N., and Cooke, R. (1995) *Biophys. J. 68*, 1980−1990.
39. Goodno, C. C. (1979) *Proc. Natl. Acad. Sci. U.S.A. 76*, 2620−2624.
40. Huxley, A. F., and Tideswell S. (1996) *J. Muscle Res. Cell Motil. 17*, 507−511.
41. Trybus, K. M., and Taylor, E. W. (1980*) Proc. Natl. Acad. Sci. U.S.A. 77*, 7209−7213.
42. Cantino, M. E., Allen, T. S., and Gordon, A. M. (1993) *Biophys. J. 64*, 211−222.
43. Swartz, D. R., Greaser, M. L., and Marsh, B. B. (1990) *J. Cell Biol. 111*, 2989−3001.
44. Chalovich, J. M. (1992) *Pharmacol. Ther. 55*, 95−148.

45. Zot, A. S., and Potter, J. D. (1989) *Biochemistry 28*, 6751−6756.
46. Morano I., and Ruegg, J. C. (1991) *Pflugers Arch. 418*, 333−337.
47. Ishii, Y., and Lehrer, S. S. (1990) *Biochemistry 29*, 1160−1166.
48. Wakabayashi, K., Tanaka, H., Saito H., Moriwaki, N., Ueno, Y., and Amemiya, Y. (1991) *Adv. Biophys. 27*, 3−13.
49. Grabarek Z., Grabarek J., Leavis P. C., and Gergely J., (1983) *J. Biol. Chem. 258*, 14098−14102.
50. Tobacman, L. S., and Sawyer, D. (1990) *J. Biol. Chem. 265*, 931−939.
51. Greene L. E. (1986) *J. Biol. Chem. 261*, 1279−1285.
52. Williams, D. L., Greene, L. E., and Eisenberg, E. (1988) *Biochemistry 27*, 6987−6993.
53. Hoar, P. E., Mahoney, C. W., and Kerrick, G. L. (1987) *Pflugers Arch. 410*, 30−36.
54. Millar N. C., and Homsher E. (1990) *J. Biol. Chem. 265*, 20234−20240.
55. Swartz, D. R. and Moss, R. L. (1992) *J. Biol. Chem. 267*, 20497−20506.
56. Walker J. W., Lu Z., and Moss R. L. (1992) *J. Biol. Chem. 267*, 2459−2466.
57. Haselgrove, C. (1972) *Cold Spring Harbor Symp. Quantum Biol. 37*, 341−352.
58. Huxley, H. E. (1972) *Cold Spring Harbor Symp. Quantum Biol. 37*, 361−376.
59. Parry, D. A. D., and Squire, J. M. (1973) *J. Mol. Biol. 75*, 33−55.
60. Chalovich, J. M., and Eisenberg, E. (1986) *J. Biol. Chem. 261*, 5088−5093.
61. Chalovich, J. M., Chock, P. B., and Eisenberg, E. (1981) *J. Biol. Chem. 256*, 575−578.
62. Flicker, P. F., Milligan, R. A., and Applegate, D. (1991) *Adv. Biophys. 27*, 185−196.
63. Lehman, W., Craig, R., and Vibert, P. (1994) *Nature 368*, 65−67.
64. Lorenz, M., Poole, K. J. V., Popp, D., Rosenbaum, G., and Holmes, K. C. (1995) *J. Mol. Biol. 246*, 108−119.
65. Vibert, P., Craig, R., and Lehman, W. (1997) *J. Mol. Biol. 266*, 8−14.
66. McKillop, D. F. A., and Geeves, M. A. (1993) *Biophys. J. 65*, 693−701.
67. Holmes, K. C. (1995) *Biophys. J. 68*, 2−7s.
68. Poole, K. J. V., Holmes, K. C., Evans, G., Rosenbaum, G., Rayment, I., and Lorenz, M. (1995) *Biophys. J. 68*, 348s.
69. Farah, C. S., and Reinach, F. (1995) *FESEB J. 9*, 755−767.
70. Szczesna, D., and Fajer, P. (1995) *Biochemistry 34*, 3614−3620.
71. Cassell, M., and Tobacman, L. S. (1996) *J. Biol. Chem. 271*, 12867−12872.
72. Bremel, R. D., and Weber, A. (1972) *Nature New Biol. 238*, 97−101.
73. Lehrer, S. S., and Morris, E. P. (1982) *J. Biol. Chem. 257*, 8073−8080.
74. Fajer, E. A., Ostap, E. M., Thomas, D. D., Naber, N., and Fajer, P. G. (1995) *Biophys. J. 68*, 322.

BI972062G